Mission Function Control for a Slew Maneuver Experiment

Hironori Fujii, Toshiyuki Ohtsuka, and Satoshi Udou
Tokyo Metropolitan Institute of Technology, Tokyo 191, Japan

A control algorithm named mission function control is experimentally demonstrated and verified on a slew maneuver of a flexible space structure model. The mission function control algorithm employs a Lyapunov-type function that consists of generalized energy functions. The model consists of a rigid body having a cantilevered flexible appendage; it is controlled to slew in a horizontal plane by a torque motor. Analytical study indicates that vibrational motion of the flexible appendage can be sensed by strain gauges as a bending moment and shear force at the root of the appendage. Results of the experiment show that a simple implementation of the algorithm leads to excellent controlled behavior of the slew maneuver as well as excellent control robustness.

I. Introduction

THE role of experiments is growing in parallel with the advances in numerical simulation techniques, in our quest to establish pertinent controllers for large space structures (LSS). Experimental data are essential to comprehend basic characteristics of controlled behavior of LSS and are necessary to include unknown elements into numerical simulators that exhibit only such behavior as the human can foresee. Neither the experimental nor the numerical simulation is almighty and both should be used jointly to establish and evaluate control laws for LSS in the space environment. This paper is devoted to reporting results of an experiment on controlled slew maneuvers of a model of an LSS exploited analytically and numerically in Ref. 1.

A slew maneuver is simply a control to change the attitude angle of a spacecraft from an initial one to a desired final angle.[2] A large spacecraft usually has some flexible structures whose vibrational motion is inevitably excited by the slew maneuver. Control of the slew maneuver must not only change the attitude angle of a spacecraft from one to another, but do so with minimal vibrational excitation of flexible structures throughout the maneuver and with no vibration at the end of the maneuver. The slew maneuver is usually treated as a two-point boundary-value problem specified in both the initial and final states in a prescribed time. This specification usually results in an open-loop control that would be affected seriously by disturbances and/or parameter uncertainty of the model.

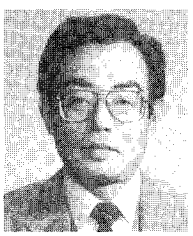

Hironori Fujii is a Professor in the Department of Aerospace Engineering at the Tokyo Metropolitan Institute of Technology. He earned his D.E. degree from Kyoto University in 1975. His research interests include dynamics and control of large space structures and robotics for aerospace application. Since 1982 he has been chairman of the Research Group on Control of Flexible Space Structures in Japan. He is a member of AIAA, the American Astronautical Society, and the Japan Society for Aeronautical and Space Sciences, and an Associate Fellow of the Canadian Aeronautics and Space Institute.

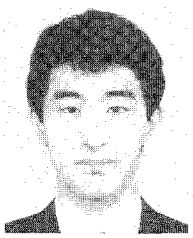

Toshiyuki Ohtsuka received a bachelor's degree in aerospace engineering in 1990, and is a Graduate Student at the Tokyo Metropolitan Institute of Technology. His research interests include control theory with application to large space structures. He is a Student Member of AIAA and the Japan Society for Aeronautical and Space Sciences.

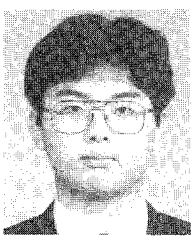

Satoshi Udou received a bachelor's degree in aerospace engineering in 1990, and is a Graduate Student at the Tokyo Metropolitan Institute of Technology. His research interests include attitude control of spacecraft. He is a Student Member of AIAA and the Japan Society for Aeronautical and Space Sciences.

Received Oct. 25, 1988; revision received May 23, 1990; accepted for publication May 28, 1990.

Several papers are devoted to experimental examination of the slew maneuver control and demonstration of the control algorithms. Breakwell and Chambers[3] tested the linear-quadratic-Gaussian algorithm for the slew maneuver on the TOYSAT structural control experimental hardware. Kida et al.[4] applied the independent dual-mode control on the slew maneuver through a ground-based hardware demonstration. Juang et al.[5] verified experimentally the validity of the linear optimal terminal control law implemented in an analog computer as applied to flexible structures for the slew maneuver. In these papers, the motion of flexible structures is described by modal models truncated to the low order of flexible motion. These control algorithms employing the modal model need an onboard computer with sufficient speed and storage to implement the variable feedback gain for sufficient retained modes in the modal model.

This paper demonstrates experimentally the applicability of the mission function control algorithm to the control on the slew maneuver of a spacecraft with a flexible appendage. The mission function control is a control algorithm presented by the first author,[6] and its validity is examined on application to the slew maneuver using numerical simulation in Ref. 1. The algorithm employs as the mathematical description of motion of a flexible structure the partial differential equation, which describes most precisely such a distributed parameter system as an LSS. This mathematical modeling evidently includes information of all modes in comparison with the case where the usual modal expansion method is applied, and is free from the crucial truncation effect on the problem. The algorithm also employs Lyapunov generalized energy functions that embody the dynamical features of LSS. This fact leads analytically to a physically meaningful reduction of the algorithm. As a consequence, the number and locations of the sensors are determined naturally to be the bending moment and shear force at the root of the flexible appendage, whereas the actuator is prescribed to be a torque motor in the central rigid body.

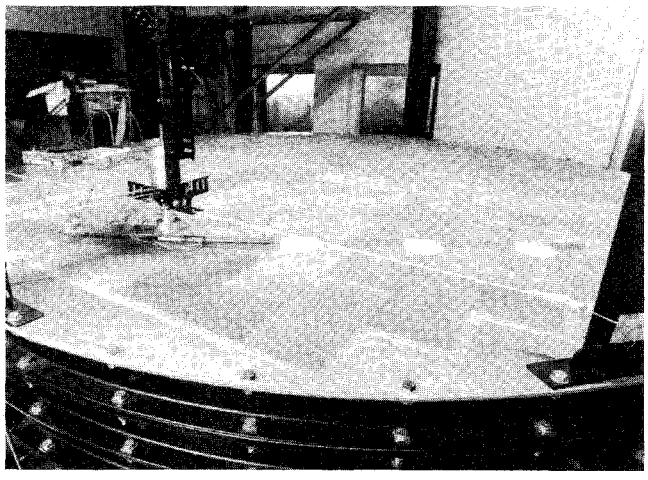

Fig. 1 Photograph and diagram of experimental setup.

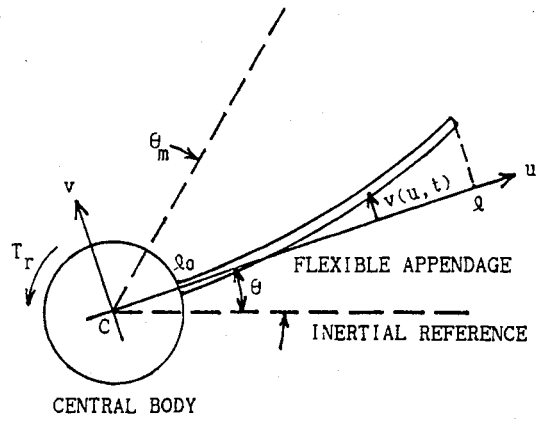

Fig. 2 System model.

It may be noted that the finite time constraint on the slew maneuver is removed in this study to close the control loop. The slew maneuver objective is to drive the system from any initial condition to allowably small errors in the final state, and this allows generation of a closed-loop control algorithm.

Results of the control experiment show a simple and practical implementation of the algorithm. The results also demonstrate robustness of the optimal regulator, leading to an excellently controlled slew maneuver.

II. Experiment Setup

The model of the flexible appendage used in this experiment is a 1150-mm-long aluminum beam with a cross section of 20×0.5 mm, as shown in Fig. 1. The beam is clamped to a rigid body that rotates in a horizontal plane through actuation of a dc torque motor. The model is set on a zero-gravity simulation table with a horizontal test surface of 3.2 m in diameter and allowed to move under no influence of the Earth's gravity. The surface of the table is made of porous metal and air taken through fans flows with velocity about 0.2 m/s from the surface to support a specimen on the table. The model beam is equipped with three 120-mm-diam circular boards made of styrene resin to receive the airflow and to move freely in the horizontal plane.

Sensing of the necessary data for the control is provided by a tachometer at the rotary shaft of the torque motor and two full-bridge strain gauges located at the beam root. The tachometer is used to measure angular velocity of the central rigid body about the rotary axis, and its output is integrated by an analog circuit to obtain the attitude angle of the central rigid body. The strain gauges are used to measure bending moment and shear force at the root of the beam. Data from these sensors are amplified and put into a digital computer, NEC PC-9801VM (CPU: 8086), through an analog-to-digital (A/D) converter. The computer processes the digital data under the control algorithm and puts out the control signal to drive the dc torque motor through a digital-to-analog (D/A) converter. The control signal is converted to electric current by a current amplifier to drive the motor. The control software is programmed in FORTRAN and in assembly language for the part operating the input/output port of the computer. The graphic presentation program is coded in BASIC. The sample interval of the control process is set to be 2.0 ms. The data obtained in the control experiment are stored temporarily in the inner memory system of the computer and transferred to an outer memory system after the experiment.

III. System Dynamics and Control Algorithm

System Model

The present system is modeled as a two-dimensional rotary motion of a rigid body equipped with a flexible beam, as

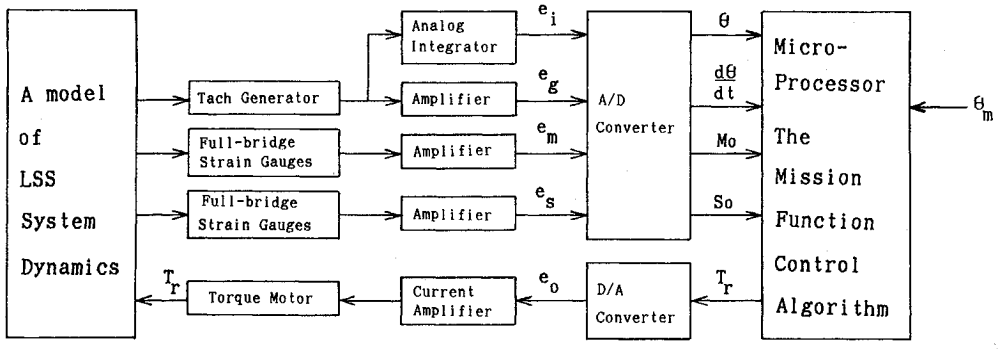

Fig. 3 Control-loop diagram.

illustrated in Fig. 2. The rigid body is actuated in the plane by the control torque T_r about the center of rotation C and the flexible beam has deflection $v(u,t)$ in the same plane. The flexible beam is assumed to be a Bernoulli-Euler beam with one end ($u=l_0$) fixed on the rigid body and the other end ($u=l$) free.

Let us neglect the mass of the support boards, the friction in the motor, and structural damping of the beam that is sufficiently small in comparison with the air drag damping. Then the behavior of the present system is described by the following equations of motion in terms of the partial differential equations (neglecting higher order terms):

$$I_r\frac{d^2\theta}{dt^2}+\int_{l_0}^{l}\rho u\left(\frac{\partial^2 v}{\partial t^2}+u\frac{d^2\theta}{dt^2}\right)du + \int_{l_0}^{l}cu\left(\frac{\partial v}{\partial t}+u\frac{d\theta}{dt}\right)du = T_r \tag{1}$$

$$\rho\left(\frac{\partial^2 v}{\partial t^2}+u\frac{d^2\theta}{dt^2}\right)+c\left(\frac{\partial v}{\partial t}+u\frac{d\theta}{dt}\right)+EI\frac{\partial^4 v}{\partial u^4}=0 \tag{2}$$

with the boundary conditions

$$v=\frac{\partial v}{\partial u}=0 \quad (u=l_0), \qquad \frac{\partial^2 v}{\partial u^2}=\frac{\partial^3 v}{\partial u^3}=0 \quad (u=l) \tag{3}$$

where θ denotes the attitude angle of the central rigid body, and I_r, ρ, EI, and c denote the moment of inertia of the central rigid body, the mass density of the beam per unit length, the bending rigidity of the beam, and the damping coefficient of the air drag, respectively. The parameters ρ, EI, and c are assumed to be constant along the beam. The air drag force is assumed to be negative proportional to velocity: $c>0$.

Mission Function Control Algorithm for Slew Maneuver

The slew maneuver is defined as an action to change the dynamical state of the system from an initial one with $\theta=\theta_0$ into a desired one (call this desired object the mission state) with

$$\frac{d\theta}{dt}=0 \tag{4a}$$

$$\theta=\theta_m \tag{4b}$$

$$\frac{1}{2}\int_{l_0}^{l}\rho\left(\frac{\partial v}{\partial t}+u\frac{d\theta}{dt}\right)^2du+\frac{1}{2}\int_{l_0}^{l}EI\left(\frac{\partial^2 v}{\partial u^2}\right)^2du=0 \tag{4c}$$

where θ_m is the desired attitude angle to be obtained (call it the mission angle), and Eq. (4c) denotes the sum of the kinetic energy and the elastic strain energy, respectively, of the beam.

Let us consider a Lyapunov function called the mission function, which is positive definite and is zero only at the mission state. If it is possible to force the time derivative of the mission function to be negative definite, the dynamical state of the system approaches the mission state. The mission function M is selected in this case as

$$2M=a_1I_r\left(\frac{d\theta}{dt}\right)^2+a_2(\theta-\theta_m)^2+b\left[\int_{l_0}^{l}\rho\left(\frac{\partial v}{\partial t}+u\frac{d\theta}{dt}\right)^2du + \int_{l_0}^{l}EI\left(\frac{\partial^2 v}{\partial u^2}\right)^2du\right] \tag{5}$$

where a_1, a_2, and b are positive weighting coefficients. As is apparent from Eq. (5), the mission function M is positive definite and is zero only at the mission state, Eqs. (4). Note that the mission function [Eq. (5)] is a Lyapunov function constructed to control a dynamic state to approach an objective state, the mission state. A specific feature of the mission function is to include such a generalized energy function as the right-hand side of Eq. (5).

Using Eqs. (1-3), the time derivative of the mission function is obtained as

$$\frac{dM}{dt}=\tilde{T}\frac{d\theta}{dt}-bc\int_{l_0}^{l}\left(\frac{\partial v}{\partial t}+u\frac{d\theta}{dt}\right)^2du \tag{6}$$

where

$$T_r=-(1/a_1)\left[-\tilde{T}+a_2(\theta-\theta_m)+(b-a_1)(l_0S_0-M_0)\right] \tag{7}$$

and $\tilde{T}$ is a freely assignable part of the control torque T_r, and M_0 and S_0 denote the bending moment and the shear force, respectively, at the root of the beam:

$$M_0=EI\frac{\partial^2 v}{\partial u^2}\bigg|_{l_0}, \qquad S_0=EI\frac{\partial^3 v}{\partial u^3}\bigg|_{l_0} \tag{8}$$

Note that the term $(M_0-l_0S_0)$ as shown in Eq. (7) denotes moment, or torque, about the center of rotation C due to vibration of the flexible beam.

The time derivative of the mission function dM/dt can be forced to be negative definite if $\tilde{T}$ is selected, for example, as

$$\tilde{T}=-k\frac{d\theta}{dt}, \qquad k>0 \tag{9}$$

Table 1 Parameters

Aluminum beam	Central body
$l=1190.3$ mm	$I_r=3.43\times10^{-2}$ kg·m²
$l_0=40.3$ mm	
$\Delta l=12.0$ mm	Current amplifier
$EI=1.48\times10^{-2}$ N·m²	$A_i=0.51$ A/V
$\rho=2.78\times10^{-2}$ kg/m	
	Conversion factors
Torque motor	$K_g=2.589$ V·s/rad
$K_t=0.042$ N·m/A	$K_i=-3.53$ V/rad
$F_v=1.232\times10^{-4}$ N·m·s/rad	$K_s=9.58$ V/N
$F_l=2.82\times10^{-5}$ N·m·s/rad	$K_m=1.60\times10^{2}$ V/(N·m)
$T_{r+}=8.0\times10^{-3}$ N·m	
$T_{r-}=5.4\times10^{-3}$ N·m	

Table 2 Control performance

Case	Fig.	Conditions (a_2,b,k)	Attitude angle: Overshoot, %	Attitude angle: Settling time, s	Maximum amplitude of bending moment, N·m
1	4a	R,[a] BB[b]	0	3.1	—
2	4b	R, MFC[c] (30,–,30)	0	2.8	—
3	5	F,[d] MFC (30,2100,0)	30	No settling	0.015
4	6	F, MFC (100,2100,40)	14	9.9	0.020
5	7	F, MFC (30,4500,40)	0	5.7	0.006
6	8	F, MFC (30,2100,40)	0	4.9	0.009
7	9	F, MFC (30,100,40)	0 (0)[e]	4.4 (3.2)	0.017 (0.023)

[a]With central rigid body only. [b]Bang-bang control.
[c]Mission function control. [d]With flexible beam. [e]Numerical result.

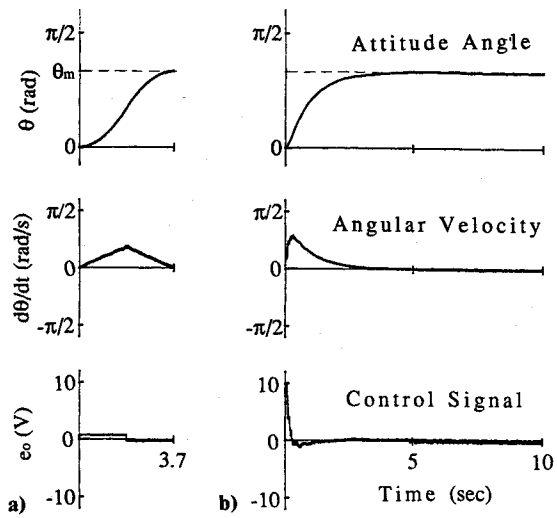

Fig. 4 Control of central rigid body without flexible appendage: a) bang-bang control; b) mission function control (a_1 = 100, a_2 = 30 N·m, k = 30 N·m·s).

Then Eq. (6) becomes

$$\frac{dM}{dt} = -k\left(\frac{d\theta}{dt}\right)^2 - bc\int_{l_0}^{l}\left(\frac{\partial v}{\partial t}+u\frac{d\theta}{dt}\right)^2 du \qquad (10)$$

which is negative definite. Thus, it is evident that the mission state is asymptotically stable and the control torque T_r will accomplish the mission if implemented through Eqs. (7) and (9) as follows.

$$T_r = -\frac{1}{a_1}\left[k\frac{d\theta}{dt}+a_2(\theta-\theta_m)+(b-a_1)(l_0S_0-M_0)\right] \qquad (11)$$

This expression of the torque is used as a control algorithm for the slew maneuver treated herein. It should be noted that the control algorithm is derived directly from the partial differential equations that describe the distributed parameter system most precisely, and it is naturally evident that sufficient data to simultaneously control the rotary motion of the central rigid body and vibration of the cantilever beam are contained in the hub rotation state (θ, $d\theta/dt$), the bending moment (M_0), and the shear force (S_0) at the root of the flexible beam.

IV. Implementation of Control Algorithm

The control-loop diagram of the present experiment is illustrated in Fig. 3. It is shown in Eq. (11) that the data to be fed back to the control torque T_r are values of θ, $d\theta/dt$, S_0, and M_0. Those data measured are fed into the computer through the following relations:

$$\frac{d\theta}{dt}=\frac{e_g}{K_g}, \quad \theta=\frac{e_i}{K_i}, \quad S_0=\frac{e_s}{K_s}, \quad M_0=\frac{e_m}{K_m} \qquad (12)$$

where e_g, e_i, e_s, and e_m are the measured output voltage of the tachometer, its analog integration, and amplified output voltages of the two full-bridge strain gauges, respectively, and K_g, K_i, K_s, and K_m are conversion factors. Among these factors, the values of K_g and K_i are determined from calibration and the remainder are calculated theoretically. These values are shown in Table 1. The shear force is obtained approximately by using a difference of the bending moments at two points. This approximation is based on the fact that the shear force is the space derivative of the bending moment; i.e., $S_0=\partial M/\partial u\,|\,l_0$. The distance between two points Δl is set to be 12.0 mm in the experiment.

The torque motor is driven by an amplified current converted from the output voltage of the D/A converter and actuates the central rigid body attached to the rotary shaft of the motor. The control torque T_r produced in the motor by the output voltage e_o of the D/A converter is expressed as

$$T_r = K_t A_t e_o - (F_v + F_l)\frac{d\theta}{dt} \qquad (13)$$

where K_t denotes the torque sensitivity of the motor, A_t the current gain of the amplifier, and F_v and F_l the viscous and loss damping coefficients in the motor, respectively. Their values are presented in Table 1.

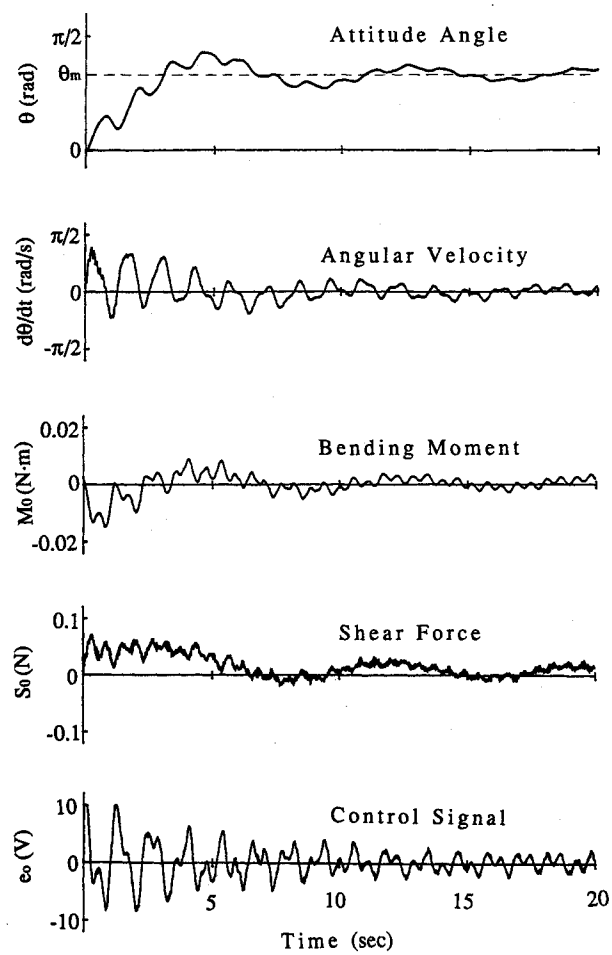

Fig. 5 System responses (a_1 = 100, a_2 = 30 N·m, b = 2100, k = 0 N·m·s).

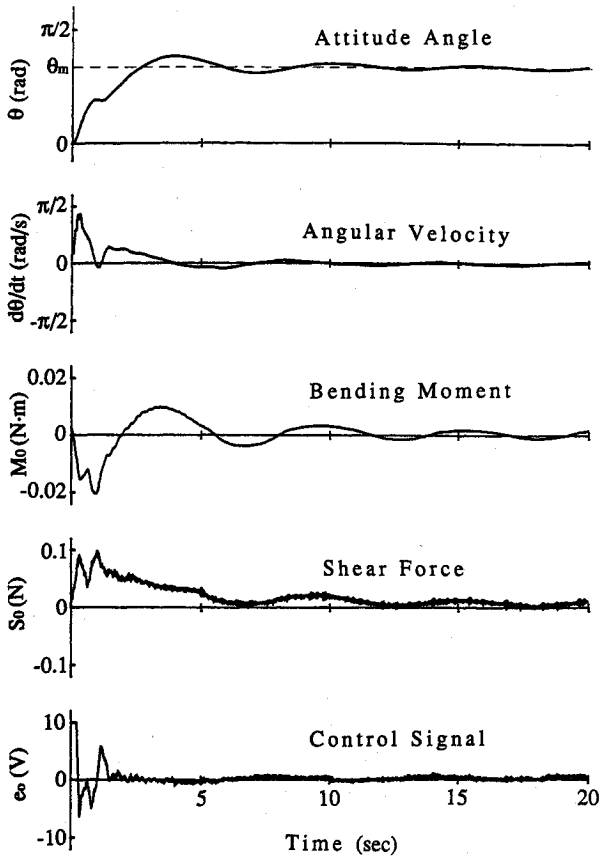

Fig. 6 System responses ($a_1 = 100$, $a_2 = 100$ N·m, $b = 2100$, $k = 40$ N·m·s).

Using Eqs. (11–13), the voltage e_o to be output through the D/A converter is determined by

$$e_o = (F_v + F_l - k/a_1)e_g/(K_g K_t A_t) - a_2 e_i/(a_1 K_i K_t A_t) - (b - a_1) l_0 e_s/(a_1 K_s K_t A_t) + (b - a_1) e_m/(a_1 K_m K_t A_t) + a_2 \theta_m/(a_1 K_t A_t) \quad (14)$$

The torque motor used in this experiment is a direct-drive type with brushes, and there exists a frictional torque. The frictional torque is canceled in this experiment by compensating for it in the coding of the control program. The coding is to add voltage corresponding to the frictional torque onto the control signal voltage calculated by Eq. (14). The compensating voltage is determined to be $e_+ = +0.375$ V when the value of $d\theta/dt$ is positive and to be $e_- = -0.250$ V when that of $d\theta/dt$ is negative after an examination on the motor characteristic. The compensating torques T_{r+} and T_{r-} are presented in Table 1 corresponding to the compensating voltages e_+ and e_-, respectively.

V. Experimental Results

The model is controlled to slew from $\theta_0 = 0$ to $\theta_m = \pi/3$ rad (60 deg) in the experiment. The value of the weighting coefficient a_1 is fixed to be 100, and values of the other coefficients are varied to investigate the effect of variation of these values on the controlled behavior of the system. Table 2 summarizes some typical features of the control performance and conditions in the experimental results. The overshoot and settling time of the attitude angle are used to specify performance of the control of the attitude angle. The overshoot is measured in terms of the percentage of the deviation of the attitude angle over the mission angle. The settling time of the attitude angle is defined here as the time necessary to settle the attitude angle into the range within ±5% of the mission angle. The maximum amplitude of the bending moment at the root of the beam can be considered a measure of the intensity of vibrational excitation in the flexible beam.

First, open-loop bang-bang control is examined for the control of the rigid model without including the flexible appendage in order to show the validity of the compensation of the frictional torque. The response of the bang-bang control and the response of the mission function control are shown in Fig. 4. This figure indicates transient responses with respect to time of the attitude angle θ, the angular velocity of the central rigid body $d\theta/dt$, and the control signal voltage e_o.

The bang-bang control applies positive and negative torque of equal amplitude for equal intervals of time to the central rigid body. The time interval of the torque actuation is estimated after solution of the equation of motion, which does not include the frictional torque. The central rigid body is driven to the mission angle in 3.7 s by the applied torque of ±0.012 N·m for the present case (see Fig. 4a). The settling time of the attitude angle is 3.1 s (see Table 2). The amplitudes of the positive control signal and of the negative control signal in the bang-bang control do not have the same value due to the compensation of the frictional torque. The actual torque applied to the central rigid body is proportional to the value of the control signal voltage reduced by the compensating voltage of the frictional torque.

The mission function control is identical to the well-known proportional-differential control when the control is applied on the attitude angle of the central rigid body without the flexible appendage. This will be recognized easily since the mission function [Eq. (5)] is expressed in this case without the third term representing the energy of the flexible beam. The settling time of the attitude angle is 2.8 s for the results in Fig. 4b.

Next, the results are introduced for the slew maneuver experiment on the model equipped with the flexible beam. The

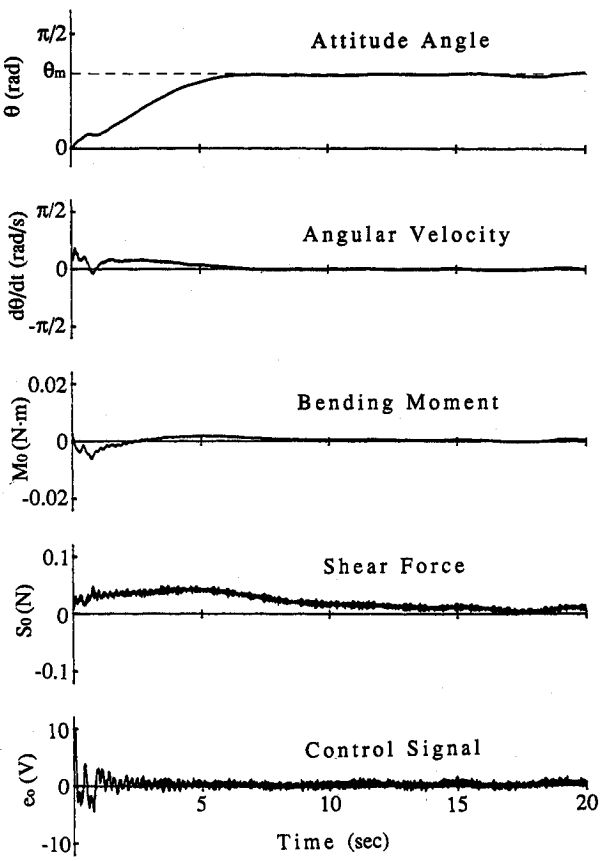

Fig. 7 System responses ($a_1 = 100$, $a_2 = 30$ N·m, $b = 4500$, $k = 40$ N·m·s).

system responses are shown in Figs. 5–9 for some sets of values of the weighting coefficients. These figures indicate transient responses of the model with respect to time in the attitude angle θ, the angular velocity of the rigid body $d\theta/dt$, the bending moment at the root of the beam M_0, the shear force at the root of the beam S_0, and the control signal voltage e_o.

Figure 5 shows the results of the case with the following values of the weighting coefficients: $a_1 = 100$, $a_2 = 30$ N·m, $k = 0$ N·m·s, and $b = 2100$. As is apparent from Eq. (10), the mission function decreases in the case with $k = 0$ not by the active control motion but by the passive air drag damping and other energy losses in the system. The results in Fig. 5 are to show the contribution of the passive damping to the present slew maneuver. The overshoot of the attitude angle is 30% and the maximum amplitude of the bending moment is 0.015 N·m. The attitude angle does not settle to the mission angle within 20 s. Saturation of the control signal voltage is observed for the initial period of 0.1 s in the control process.

Figure 6 presents the controlled behavior of the system with the nonzero coefficient $k = 40$ N·m·s. The overshoot and the settling time of the attitude angle are 14% and 9.9 s, respectively. The maximum amplitude of the bending moment is 0.020 N·m. It is observed in this case that the initial control signal voltage saturates for the initial period of 0.2 s, since the large value of the weighting coefficient a_2 causes an excessive control signal voltage.

The coefficient a_2 is decreased to 30 N·m and the coefficient b is increased to 4500 in the case shown in Fig. 7. The attitude angle reaches the mission angle with a settling time of 5.7 s and with no overshoot. The maximum amplitude of the bending moment is 0.006 N·m, i.e., 30% of that obtained in Fig. 6.

Results are shown in Fig. 8, where the coefficient b is decreased to 2100. The settling time of the attitude angle is 4.9 s and is 86% of the result shown in Fig. 7. The maximum amplitude of the bending moment is 0.009 N·m and 150% of that obtained in Fig. 7.

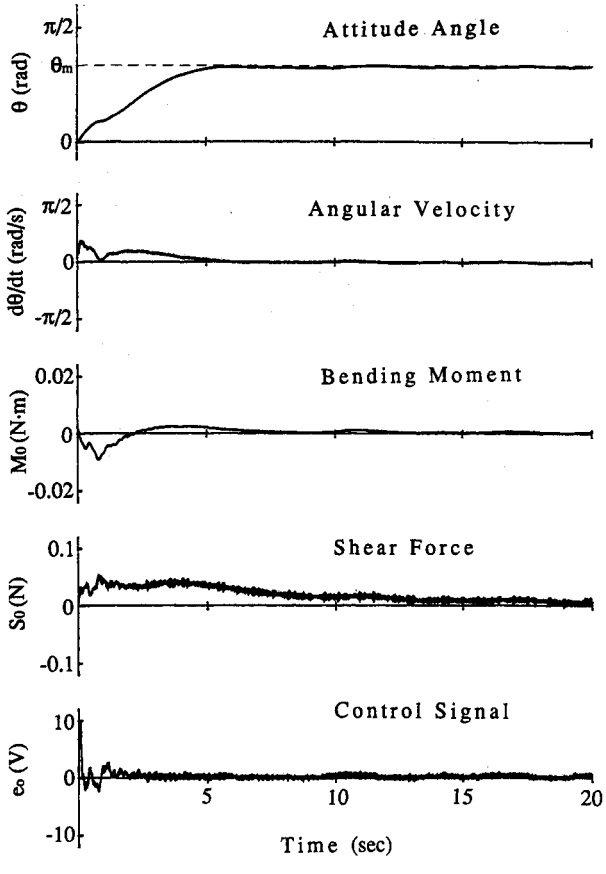

Fig. 8 System responses ($a_1 = 100$, $a_2 = 30$ N·m, $b = 2100$, $k = 40$ N·m·s).

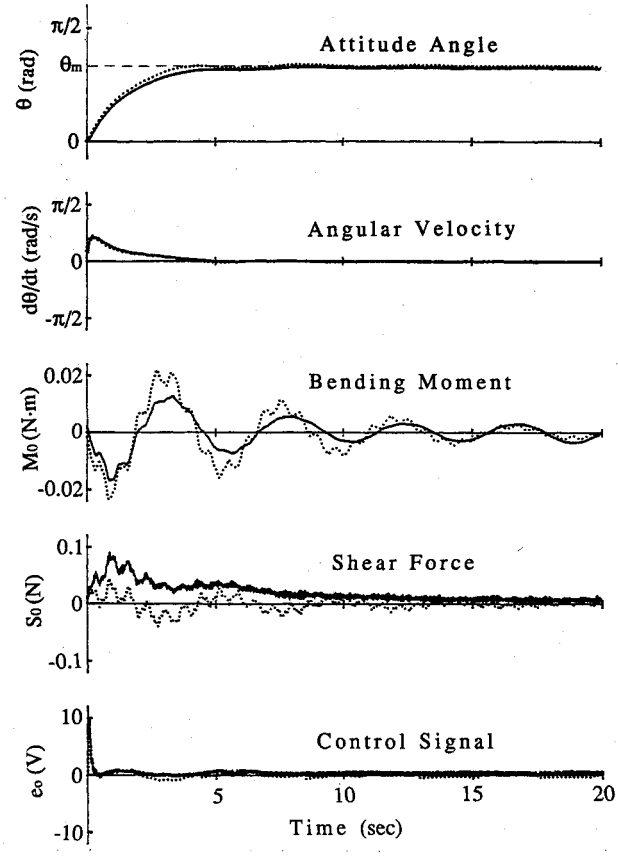

Fig. 9 System responses ($a_1 = 100$, $a_2 = 30$ N·m, $b = 2100$, $k = 40$ N·m·s). Results of numerical simulation (...) and experiment ( ).

As is easily seen from Eq. (11), the measurements of the shear force and the bending moment at the root of the beam are not fed back to the control torque in the case when the value of the coefficient b is equal to that of a_1. The last figure, Fig. 9, presents results for the case with $a_1 = b = 100$, $a_2 = 30$ N·m, and $k = 40$ N·m·s. It may be interesting here to compare the present results of the experiment with those obtained from a numerical simulation using finite-difference equations.[1] The results of a numerical simulation are shown superimposed as dotted lines on the experimental results in Fig. 9. No overshoot is seen in either the experiment or the numerical simulation. The settling time of the attitude angle in the experiment is 4.4 s, the least among the preceding cases with the flexible beam, but the maximum amplitude of the bending moment increases to 0.017 N·m. The settling time and the maximum amplitude of the bending moment in the numerical result are 3.2 s and 0.023 N·m, respectively. As expected, Fig. 9 shows a rather good agreement between those results obtained by the present experiment and the numerical simulation. The slight difference between both results is because the mathematical model of the damping does not describe the actual damping effect accurately. It may be noted from the figure that the sensor signal measuring the shear force is small as a result of the space derivative of the bending moment.

VI. Discussion

The relation between setting of values of the weighting coefficients and the controlled behavior meant in the mission function control algorithm is discussed in Ref. 1. Such an analysis is confirmed as the results of the present experiment.

An increase of the values of the coefficients a_2 and b enhances the significance of the corresponding generalized energy term in the mission function. This means that the value of the enhanced term decreases relatively faster in comparison with the values of the other terms in the control process leading to either the attitude angle θ reaching the mission angle more

rapidly or the dynamic energy of the flexible beam being dissipated faster.

The value of the coefficient k influences the control response in a more complicated manner than the other coefficients do. As is seen from Eq. (10), the time derivative of the mission function includes a term proportional to $(d\theta/dt)^2$ multiplied with the coefficient $-k$. It may be said that a rather large value of k is preferable to decrease the value of the mission function. If the value of k is too large, however, the mission function does not decrease faster because $-k/a_1$ is also the feedback gain of the angular velocity $d\theta/dt$ [Eq. (11)] and the value of $(d\theta/dt)^2$ consequently is reduced.

As discussed earlier, associated with Fig. 9, the control algorithm does not include M_0 and S_0 in the feedback variable when b is equal to a_1, as is observed from Eq. (11). In other words, the simplest controller for the slew maneuver can be implemented with the hub rotation state feedback only. This fact can be recognized easily since the mission function M [Eq. (5)] includes the Hamiltonian H of the system and is specifically written, if $a_1 = b$, as

$$2M = a_1(=b)H + a_2(\theta - \theta_m)^2 \tag{15}$$

where the Hamiltonian represents a natural mission function (see Refs. 1 and 6). Note, however, that the experimental results show that vibration of the flexible beam is not suppressed sufficiently when b is equal to a_1 (Fig. 9) in comparison with the cases when b is larger than a_1 (Figs. 7 and 8).

There are some special features inherent in the experiment and are discussed in what follows. One of them is the frictional torque in the torque motor. The responses in Fig. 4a show that the frictional torque can be canceled successfully by the simple compensation to add constant voltage onto the control signal voltage.

The others are time delay of the controller and sensor noise, especially in the sensor of the shear force. They cause a certain limit under which any particular weighting coefficient can be swept. High gain feedback over this limit leads to divergent oscillation of the system, whereas ideal implementation of the control algorithm guarantees stability for any set of positive weighting coefficients.

Another special feature of the experiment is saturation of the control signal voltage (see Figs. 5 and 6). Saturation occurs only for an initial period of the control process. It may be said therefore that it does not seriously affect the control performance.

VII. Conclusions

The mission function control algorithm applied to the slew maneuver of a spacecraft model with a flexible appendage is demonstrated experimentally . The experimental results lead to the following conclusions:

1) The partial differential equations are seen to describe the vibrational motion of the flexible appendage in a good manner to follow the analytical reduction of the mission function control algorithm. Excitation of vibration of the flexible appendage is seen to be well controlled in the experiment.

2) It is verified experimentally that sufficient information of motion of the flexible appendage can be obtained by sensing the bending moment and shear force at the root of the flexible appendage, and the vibration of the flexible appendage can be controlled by a torque in the rigid central body as is shown in the analysis of the mission function control algorithm.

3) The controlled behavior is affected critically by the sensor/actuator dynamics. Such nonlinear characteristics of the actuator and sensors as the frictional torque of a torque motor and noise in the sensors play an important role in the experimental implementation of a control algorithm. The cancellation of the frictional torque of the motor is a useful means to improve the control performance in the experiment.

4) The mission function control algorithm is regarded as a type of Lyapunov method for a mechanical system combined with the control system. It is assured experimentally that the present control algorithm has such a preferable feature as robustness of the optimal regulator leading to an excellently controlled behavior with no spillover effect.

Acknowledgments

The authors would like to thank Y. Ohkami, T. Kida, and I. Yamaguchi at the National Aerospace Laboratory for their support in conducting this work. The authors are also grateful to the reviewer, J. L. Junkins, for his encouragement. Note that Junkins et al.[7] have presented a refined control algorithm based on such a Lyapunov control design approach. Their algorithm extends the present algorithm to achieve near-minimum-time control of the flexible vehicles.

References

[1]Fujii, H., and Ishijima, S., "Mission Function Control for Slew Maneuver of a Flexible Space Structure," *Journal of Guidance, Control, and Dynamics,* Vol. 12, No. 6, 1989, pp. 858-865.

[2]Strunce, R. R., Jr., and Turner, J. D., "Enabling Technology for Large Space Systems," *Large Space Antenna Systems Technology—1982,* NASA CP 2269, 1982, pp. 601-624.

[3]Breakwell, J. A., and Chambers, G. J., "The TOYSAT Structural Control Experiment," *Journal of the Astronautical Sciences,* Vol. 31, No. 3, 1983, pp. 441-454.

[4]Kida, T., Yamaguchi, I., Ohkami, Y., Hirako, K., and Soga, H., "An Optimal Slewing Maneuver Approach for a Class of Spacecraft with Flexible Appendages," *Acta Astronautica,* Vol. 13, No. 6/7, 1986, pp. 331-318.

[5]Juang, J.-N., Horta, L. G., and Robertshaw, H. H., "A Slewing Control Experiment," *Journal of Guidance, Control, and Dynamics,* Vol. 9, No. 5, 1986, pp. 599-607.

[6]Fujii, H., and Ishijima, S., "The Mission Function Control for Deployment and Retrieval of a Subsatellite," *Journal of Guidance, Control, and Dynamics,* Vol. 12, No. 2, 1989, pp. 243-247.

[7]Junkins, J. L., Rahman, Z. H., and Bang, H., "Near-Minimum-Time Control of Distributed Parameter Systems: Analytical and Experimental Results," *Journal of Guidance, Control, and Dynamics,* Vol. 14, No. 2, 1991, pp. 406-415.